ACS APPLIED MATERIALS & INTERFACES

Letter

www.acsami.org

Preparation of an Amide Group-Connected Graphene–Polyaniline Nanofiber Hybrid and Its Application in Supercapacitors

Liu Jianhua,*[,†] An Junwei,[†] Zhou Yecheng,[‡] Ma Yuxiao,[†] Li Mengliu,[†] Yu Mei,[†] and Li Songmei[†]

[†]School of Materials Science and Engineering, Beihang University, 100191, Beijing, China

[‡]State Key Laboratory of Applied Organic Chemistry, College of Chemistry and Chemical Engineering, Lanzhou University, 730000 Lanzhou, Gansu, China

Supporting Information

ABSTRACT: Polyaniline (PANI) nanofiber is grafted onto graphene to obtain a novel graphene-polyaniline (GP) hybrid. Graphene is activated using $SOCl_2$ and reacts with PANI to form an amide group that intimately connects graphene and PANI. The existence of the amide group and its anchoring effect in the GP hybrid are confirmed and characterized by SEM, TEM, FT-IR, Raman, XPS and quantum chemistry analyses. Electrochemical tests reveal that the GP hybrid has high capacitance performances of 579.8 and 361.9 F g^{-1} at current densities of 0.3 and 1 A g^{-1}. These values indicate superiority to materials interacted by van der Waals force. Long-term charge/discharge tests at high current densities show that the GP hybrid preserves 96% of its initial capacitance, demonstrating good electrochemical stability. The improved electrochemical performance suggests promising application of the GP hybrid in high-performance supercapacitors.

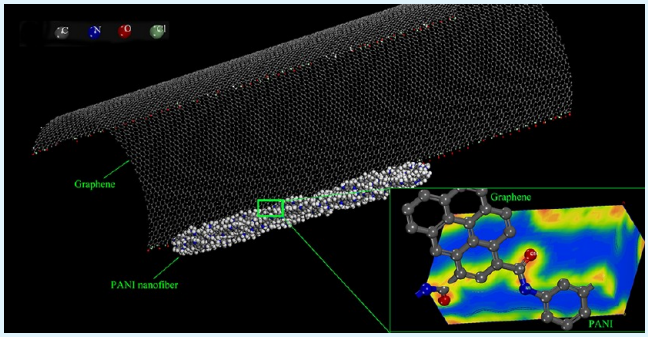

KEYWORDS: *graphene, polyaniline nanofiber, amide, supercapacitor*

1. INTRODUCTION

Supercapacitors have recently attracted significant attention.[1−3] Electrical double layer (EDL) capacitance and pseudocapacitance are two different energy storage mechanisms in supercapacitors.[4] Carbon-based materials such as carbon nanotubes[5,6] and graphene[7,8] are commonly first choices for EDL capacitors because of their high specific surface areas. On the other hand, pseudocapacitors undergo reversible faradic reactions.[9−12] Conductive polymers such as polyaniline (PANI) and polypyrrole have been applied and found to display high capacitances.

To achieve high capacitance, graphene and PANI must be comprehensively utilized. Graphene/polyaniline composites have been synthesized, applied in supercapacitors,[13−17] and found to have good capacitances. For example, Wu et al.[13] used in situ polymerization to prepare graphene/PANI composites whose capacitance is as high as 480 F·g^{-1} at a current density of 0.1 A g^{-1}. They also fabricated surfactant-stabilized graphene/PANI nanofiber composites[18] that showed a high specific capacitance of 526 F g^{-1} at 0.2 A g^{-1} and good cycling stability. Using the physical mixing method, a graphene/polyaniline film that showed a capacitance of 210 F g^{-1} at 0.3 A g^{-1} has been prepared.[17]

In previously reported graphene–polyaniline composite materials, van der Waals forces enable the interaction between graphene and PANI. On the other hand, the chemical bond, which is stronger than van der Waals forces, can make the interaction between graphene and PANI more intimate. This intimacy results in decreased interfacial resistance and improved the electrochemical performance.[19] A chemical-bonded graphene–polyaniline hybrid in which a carboxylic acid ester group connects graphene and PANI was recently reported by Kumar.[20] Unlike previous methods,[13,16,17] a novel route for obtaining a graphene-polyaniline (GP) hybrid by grafting PANI onto graphene with an amide group is proposed in the present work. The amide group not only intimately connects graphene and PANI intimately, but also acts as an electron bridge that connects the π-conjugated PANI and graphene. Consequently, a larger-scale $\pi-\pi$ conjugated system is formed. This $\pi-\pi$ conjugated structure allows faradic charges to be transferred effectively through the highly conductive graphene. The charges are prevented from accumulating, consequently decelerating the deterioration of the structure conformation of PANI with repeated ion exchange.[21] The facility of charge transfer and decreased resistance between graphene and PANI improve the electrochemical stability of the GP hybrid. Hence, a rapid charge–discharge characteristic at high sweeping rate was achieved.

The oxygen-containing groups of graphene were reduced with the carbonyl group preserved[22] using hydrazine. The obtained chemically reduced graphene sheets (CRGS) were activated using thionyl dichloride ($SOCl_2$) to obtain a graphene

Received: April 16, 2012
Accepted: May 29, 2012
Published: May 29, 2012

derivative that contained acyl chloride groups.[23] These acyl chloride groups reacted with the amine groups of PANI to form amide groups that anchored PANI nanofibers onto the graphene sheets. Figure 1 is the structural model of the GP hybrid and Figure S1 (Supporting Information) is the schematic illustration of the preparation process.

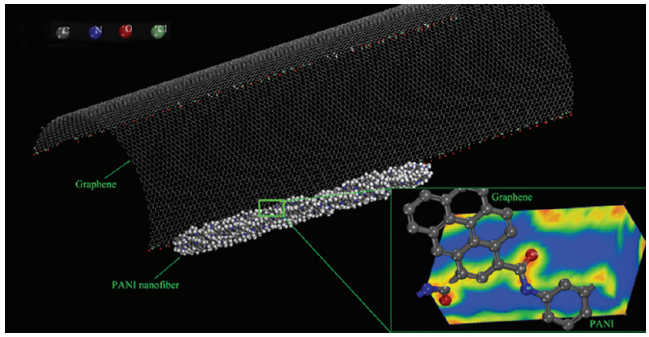

Figure 1. Structure model of GP hybrid.

2. EXPERIMENTAL SECTION

The details of the preparation of GO, CRGS, GDS, PANI nanofiber, and the GP hybrid are provided in the Supporting Information.

General Characterizations. TEM, SEM, and FT-IR were used, as well as the XPS, Raman spectrometer. The calculations are performed with the GAUSSIAN 09 package.

Electrochemical Properties Measurements. A three-electrode system was used to evaluate the electrochemical performance by CV, and galvanostatic charge−discharge techniques.[13] The detail measurement information is shown in the Supporting Information.

3. RESULTS AND DISCUSSION

3.1. Morphology and Structure. The SEM and TEM images of the GP hybrid, CRGS, and PANI are shown in Figure 2. Images a and b in Figure 2 demonstrate a homogeneous structure of the GP hybrid. Images c and d in Figure 2 exhibit the typical features of graphene and PANI nanofiber, consistent with the characteristics revealed in literature.[16,24] Figure 2e shows the good distribution of PANI nanofibers and graphene sheets in the GP hybrid, in which the nanofiber structure of PANI inhibits the agglomeration of graphene sheets. The high-resolution TEM image (Figure 2f) reveals an intimate interaction between graphene and PANI nanofiber. This intimate interaction is highly desirable for reducing the interfacial resistance between graphene and PANI, and is expected to improve the electrochemical stability of GP.[19]

To confirm the presence of amide group that connects graphene and PANI nanofiber, we carried out the FT-IR spectrum measurement of the GP hybrid (shown in Figure S2

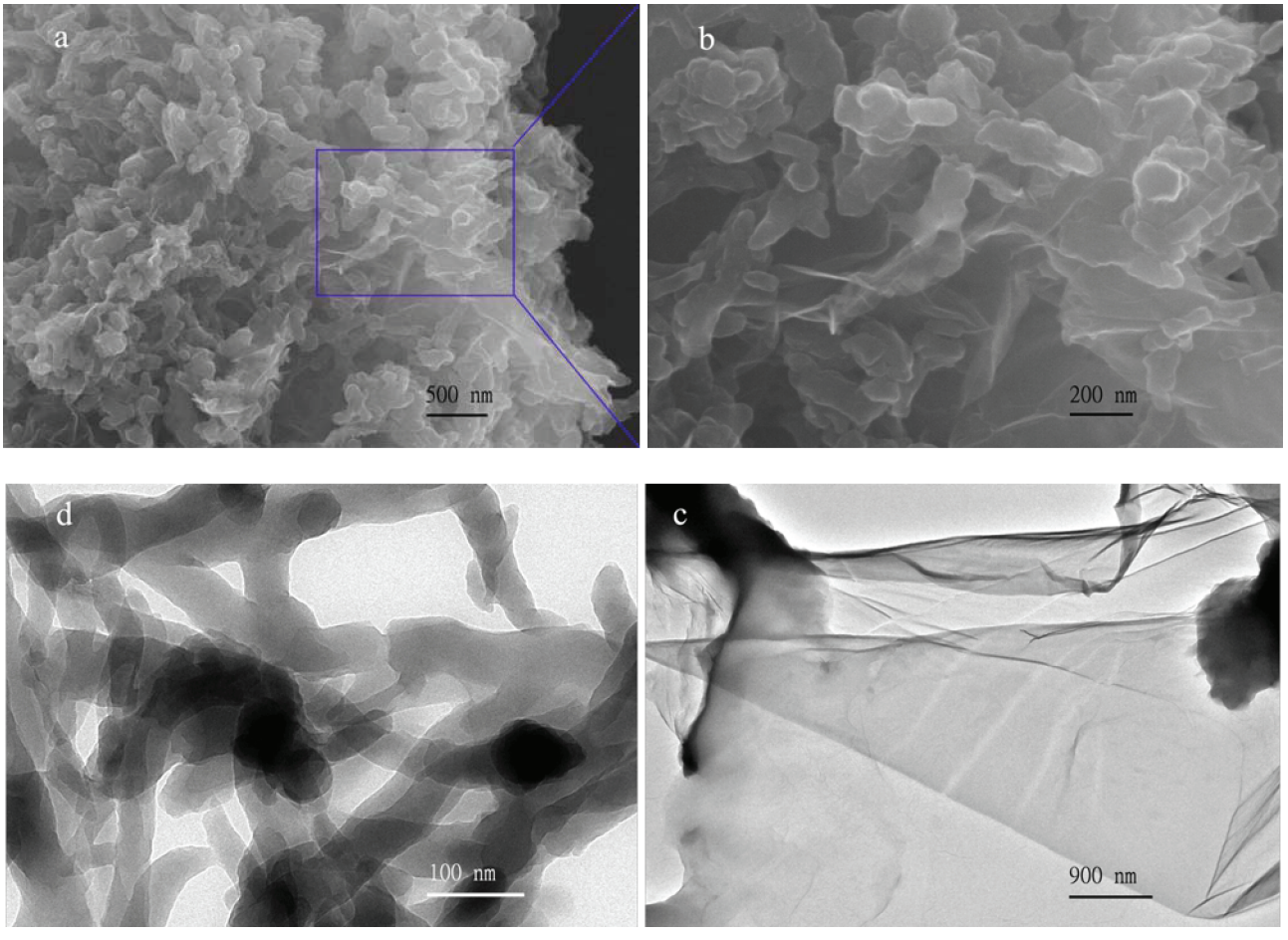

Figure 2. (a, b) SEM images of GP. TEM images of (c) CRGS, (d) PANI, and (e, f) GP.

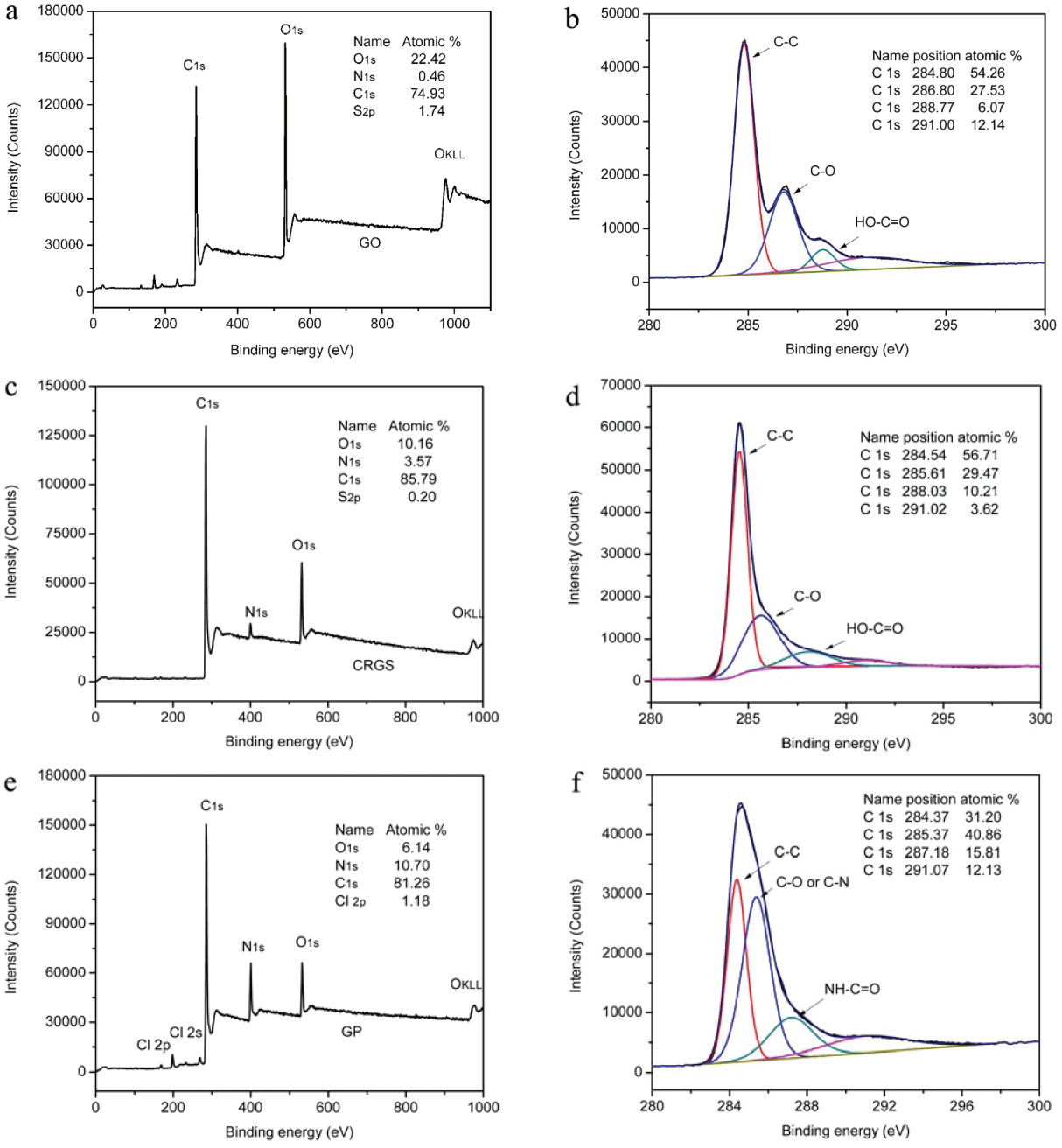

Figure 3. XPS spectra: (a, b) GO, (c, d) CRGS, (e, f) GP.

in the Supporting Information). A peak located at 1661 cm^{-1} is attributed to the C═O stretching vibration of the amide group.[25] This finding suggests the existence of amide groups in the GP hybrid as a result of the condensation reaction between PANI and activated CRGS.[23,26] The characteristic peaks at 1593, 1461, 1383, and 1221 cm^{-1} demonstrate the presence of PANI in the GP hybrid, in agreement with a previous report.[27]

The XPS spectra of GO, CRGS, and the GP hybrid are shown in Figure 3. Spectral analysis further verifies the presence of amide groups in the GP hybrid. Figure 3a reveals that the amount ratio of C:O in GO is 74.9:22.4. In Figure 3b, a peak at 288.77 eV is assigned to the carboxyl group.[28] The spectrum of CRGS in Figure 3c shows that the amount ratio of C:O is 85.79:10.16, higher than that of GO. This finding is attributed to the elimination of oxygen-containing groups in the reduction process. The presence of a peak centered at 288.03 eV demonstrates the preservation of the carboxyl group in CRGS (Figure 3d).[22] Notably, the spectrum of the GP hybrid in Figure 3e shows that the content of N is higher than that of CRGS, which confirms the presence of PANI in the GP hybrid. For the C 1s spectrum of the GP hybrid in Figure 3f, the peak centered at 287.18 eV is assigned to amide groups.[28] It is about 1 eV lower than that of the carboxyl group in GO and CRGS. The absence of a peak around 288.03 eV and the presence of a peak centered at 287.18 eV demonstrate the elimination of carboxyl groups and confirm the formation of amide groups in the GP hybrid.

The Raman spectrum in Figure S3 in the Supporting Information confirms the intimate interaction between graphene and PANI in the GP hybrid. The spectrum of CRGS shows two dominant peaks at 1362 and 1591 cm^{-1}, corresponding to the well-documented D and G bands of

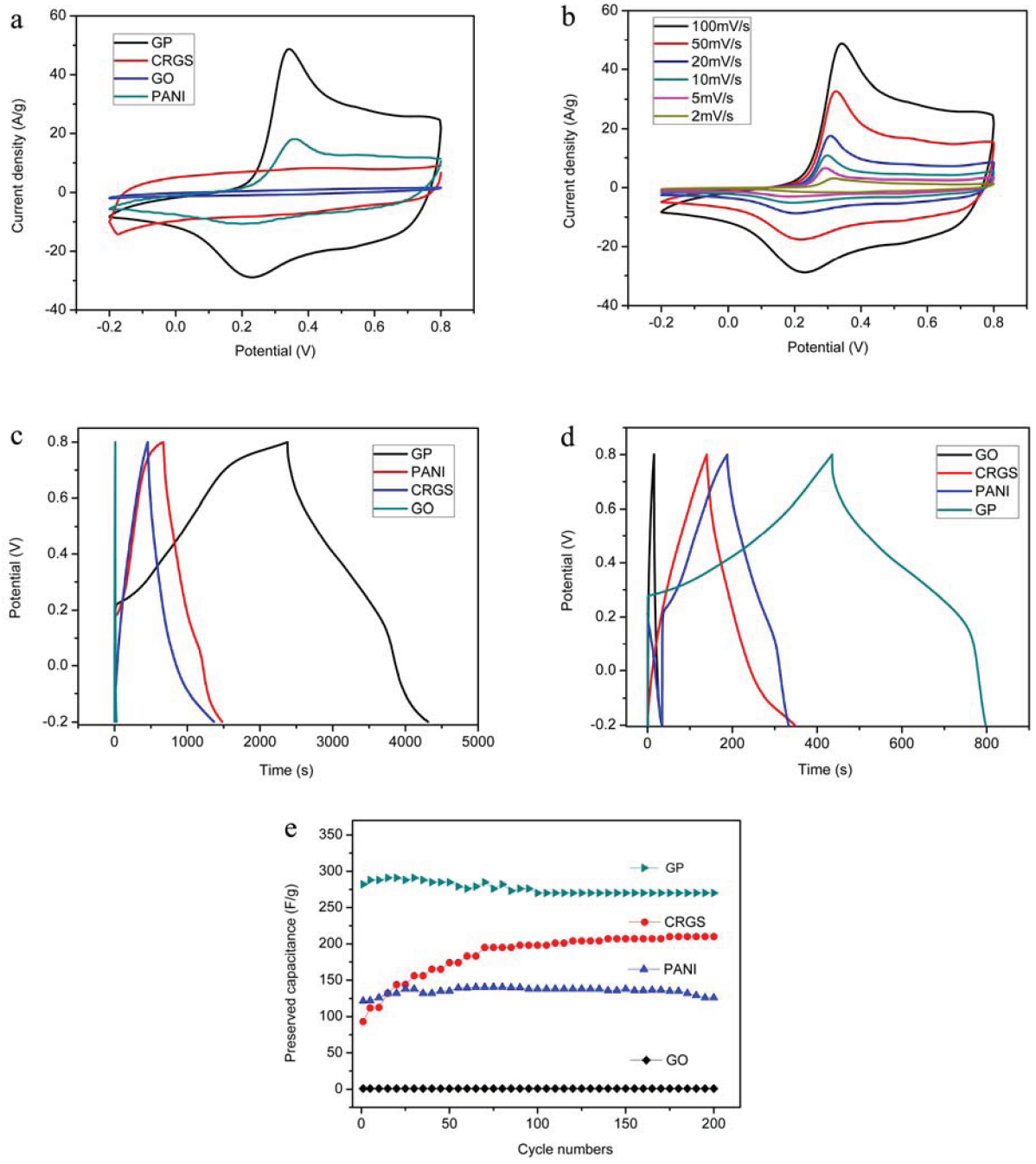

Figure 4. Electrochemical tests: (a) CV curves at 100 mV s^{-1}, (b) at different sweeping rates, (c) charge/discharge curves at 0.3 A g^{-1}, (d) at 1 A g^{-1}, (e) preserved specific capacitance at 3 A g^{-1}.

graphene,[29] respectively. For the PANI spectrum, the assignments of the characteristic bands are shown in Table S1 (see the Supporting Information). The spectrum of the GP hybrid comprises the characteristic bands of both graphene and PANI. The peaks at 1585 and 1352 cm^{-1} are identical to those of CRGS, and the peaks at 1592, 1502, 1476, 1406, 1352, 1263, 1193, and 980 cm^{-1} are attributed to PANI. However, compared with the spectrum of CRGS, the intensity ratio of the G to D bands in the GP hybrid increases. This finding demonstrates the influence of PANI on graphene due to the intimate interaction between them, consistent with previous results.[19] Several blue shifts notably occur in the spectrum of the GP hybrid compared with that of pure PANI. For example, the peak at 1502 cm^{-1} shifts from 1495 cm^{-1}, the peak centered at 1476 cm^{-1} shifts from 1464 cm^{-1}, the peak centered at 1352 cm^{-1} shifts from 1342 cm^{-1}, and the peak centered at 1263 cm^{-1} shifts from 1240 cm^{-1}. These blue shifts also reflect the intimate interaction between the π-conjugated structure of PANI and the graphene basal plane.

3.2. Supercapacitor Characterization. Electrochemical tests were carried out using cyclic voltammetry (CV) and galvanostatic charge−discharge techniques to measure the electrochemical performance of the GP hybrid. In Figure 4a, a pair of redox peaks appears in the CV curves of PANI and the GP hybrid owing to the redox converting procedures.[17] The CV curves of GO and CRGS are featureless compared with

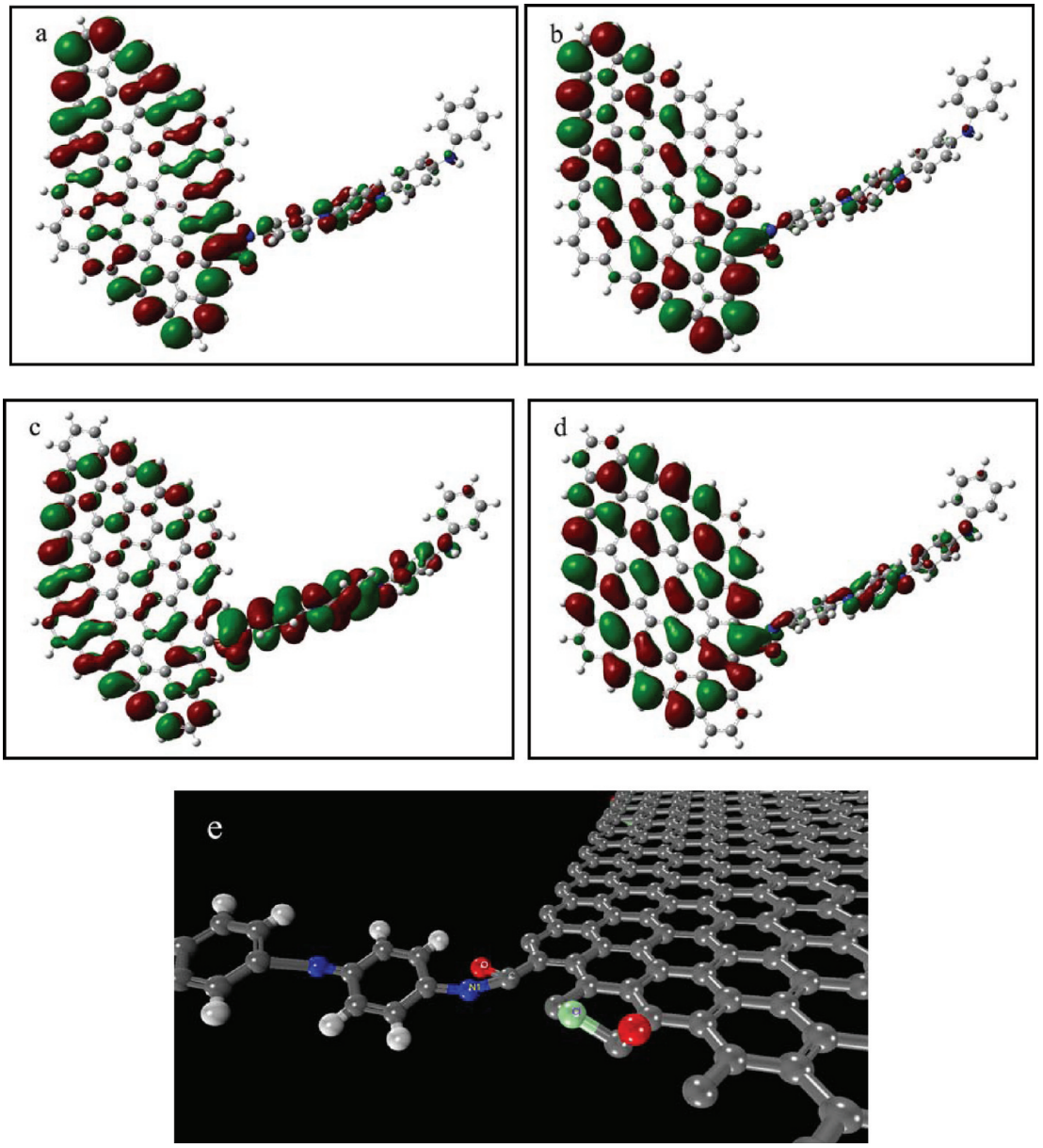

Figure 5. Structure model and frontier molecular orbitals of GP. (a) LUMO, (b) HOMO, (c) LUMO-1, (d) HOMO-1, (e) GP model.

PANI, which can be attributed to their EDL energy storage mechanism. Notably, the CV curve of the GP hybrid has a larger area than those of CRGS and PANI, indicating the higher capacitance of the GP hybrid. The CV curves of the GP hybrid at different sweeping rates were also obtained (Figure 4b). The features of the GP hybrid curve at high sweeping rates are similar to those at low ones. This high-capacitance response even with increased voltage scanning rates suggests enhanced electronic transport in the GP hybrid.[19] This enhancement is due to the intimate interaction resulting from the chemical bond between graphene and PANI.

Panels c and d in Figure 4 show the galvanostatic charge/discharge curves at current densities of 0.3 and 1A g^{-1}. The specific capacitances of the GP hybrid, PANI and CRGS calculated from their charge/discharge curves are listed in Table S2 (see the Supporting Information). Panels c and d in Figure 4 show that the specific capacitances of the GP hybrid are higher than those of PANI and CRGS. At a current density of 0.3 A g^{-1}, the specific capacitance of the GP hybrid (579.8 F·g^{-1}) is much higher than that of the graphene/polyaniline composite (210 F g^{-1} at 0.3 A g^{-1}) interacted by van der Waals force.[17] At a current density of 1 A g^{-1}, the capacitance of the GP hybrid is 361.9 F g^{-1}, higher than that of graphene-polyaniline composite (about 250 F g^{-1} at 1 A g^{-1}) connected by van der Waals force reported in literature.[16] These results suggest that the chemical bond of PANI and graphene via amide groups greatly promotes the capacitance performance of the GP hybrid.

To study the electrochemical stability of the GP hybrid, we measured the preserved specific capacitance of the GP hybrid upon 200 charge/discharge cycles at a current density of 3 A g^{-1}. As shown in Figure 4e and Table S2 in the Supporting Information, the preserved specific capacitance of the GP hybrid after 200 charge/discharge cycles is 270 F g^{-1}, conserving 96% of its original capacitance (282 F g^{-1}). Thus, good electrochemical stability is demonstrated. The preserved capacitance of the GP hybrid is also higher than those of PANI (126 F g^{-1}) and CRGS (210 F g^{-1}). This result demonstrates that the chemical anchoring effect promotes electrochemical

stability at high current densities and exerts a synergistic effect. The preserved specific capacitance of the GP hybrid is higher than those values reported by Xu[16] (227 F g^{-1} at 2 A g^{-1}) and Wu[17] (197 F g^{-1} at 3 A g^{-1}). These findings suggest that grafting PANI onto graphene with an amide group combines the advantages of the EDL capacitance of CRGS and pseudocapacitance of PANI.

To determine the mechanism of performance improvement of the GP hybrid, we developed a model of this hybrid (Figures 5e) and its electron distribution was calculated[30] (Figure 5). The LUMO and HOMO of the GP hybrid (Figures 5a,b) show that $\pi-\pi$ conjugated electrons are distributed throughout the entire GP hybrid model. Hence, a large-scale $\pi-\pi$ conjugation system comprising graphene and PANI is formed. To further investigate the effect of the amide groups on the GP hybrid, we show the electron distribution in the LUMO-1 and HOMO-1 of the GP hybrid in panels c and d in Figure 5. The electrons participating in the $\pi-\pi$ conjugation also extend to the entire conjugation system owing to the connection of the amide group. Thus, the amide group plays a significant electron-bridge role between graphene and PANI to facilitate the faradic charge transfer of PANI to graphene. The $\pi-\pi$ conjugated structure enables the charges produced by the faradic reaction of PANI to be transferred effectively through the highly conductive graphene. Notably, the conductivity of GP is about 20 times higher than that of pure PANI, which is attributed to the existence of graphene. The conductivities are listed in Table S2 (see the Supporting Information). The structure prevents the charges from accumulating, consequently decelerating the deterioration of the structure conformation of PANI with repeated ion exchange.[21] The connection made by amide groups, which is stronger than that made van der Waals forces, confers more intimacy to the interaction between graphene and PANI, as confirmed by Raman spectrum analysis. This intimacy reduces the interfacial resistance between graphene and PANI. The facility of charge transfer as well as the decreased resistance between graphene and PANI improve the electrochemical stability and realize high-capacitance response characteristics at high sweeping rates.[19] These phenomena are confirmed by the electrochemical performance test.

4. CONCLUSION

A method was proposed to obtain a novel GP hybrid connected by amide groups. Morphological characterizations by SEM and TEM reveal that in the GP hybrid, the PANI nanofibers and graphene sheets are homogeneously dispersed. FT-IR and XPS spectrum analyses confirm the existence of amide groups in the GP hybrid. Raman spectrum analysis verifies the intimate interaction between graphene and PANI in the GP hybrid. The CV curve of the GP hybrid has a larger area than those of CRGS and PANI and exhibits rapid capacitive response characteristics. The results of the galvanostatic charge/discharge tests illustrate the higher specific capacitances of the GP hybrid than previously reported conventional graphene/PANI composites interacted by van der Waals force. The preserved specific capacitance measurements at high current densities indicates the good electrochemical stability of the GP hybrid and illustrates a synergic effect. The calculated electron distribution of the GP hybrid model shows that amide groups acts as electron-bridges between PANI and graphene to form a $\pi-\pi$ conjugated system. This system facilitates charge transfer and consequently improves electrochemical performance.

■ ASSOCIATED CONTENT

Supporting Information

Additional figures and tables (PDF). This material is available free of charge via the Internet at http://pubs.acs.org.

■ AUTHOR INFORMATION

Corresponding Author

*E-mail: liujh@buaa.edu.cn.

Notes

The authors declare no competing financial interest.

■ ACKNOWLEDGMENTS

This work has been supported by the National Natural Science Foundation of china (Project 51001007).

■ REFERENCES

(1) Zhang, Y.; Li, G. Y.; Lv, Y.; Wang, L. Z.; Zhang, A. Q.; Song, Y. H.; Huang, B. L. *Int. J. Hydrogen Energy* **2011**, *36*, 11760−11766.
(2) Biswas, S.; Drzal, L. T. *ACS Appl. Mater. Interfaces* **2010**, *2*, 2293−2300.
(3) Liu, J.; An, J.; Ma, Y.; Li, M.; Ma, R. *J. Electrochem. Soc.* **2012**, *159*, A828−A833.
(4) Zhang, Y.; Feng, H.; Wu, X. B.; Wang, L. Z.; Zhang, A. Q.; Xia, T. C.; Dong, H. C.; Li, X. F.; Zhang, L. S. *Int. J. Hydrogen Energy* **2009**, *34*, 4889−4899.
(5) Rosario-Canales, M. R.; Deria, P.; Therien, M. J.; Santiago-Avilés, J. J. *ACS Appl. Mater. Inter.* **2011**, *4*, 102−109.
(6) Wang, N.; Wu, C.; Li, J.; Dong, G.; Guan, L. *ACS Appl. Mater. Interfaces* **2011**, *3*, 4185−4189.
(7) Mou, Z. G.; Dong, Y. P.; Li, S. J.; Du, Y. K.; Wang, X. M.; Yang, P.; Wang, S. D. *Int. J. Hydrogen Energy* **2011**, *36*, 8885−8893.
(8) Wu, J. S.; Zhang, K.; Mao, L.; Zhang, L. L.; Chan, H. S. O.; Zhao, X. S. *J. Mater. Chem.* **2011**, *21*, 7302−7307.
(9) Aghazadeh, M.; Golikand, A. N.; Ghaemi, M. *Int. J. Hydrogen Energy* **2011**, *36*, 8674−8679.
(10) Zhang, Y.; Gui, Y.; Wu, X.; Feng, H.; Zhang, A.; Wang, L.; Xia, T. *Int. J. Hydrogen Energy* **2009**, *34*, 2467−2470.
(11) Jiang, J.; Liu, J.; Ding, R.; Zhu, J.; Li, Y.; Hu, A.; Li, X.; Huang, X. *ACS Appl. Mater. Interfaces* **2010**, *3*, 99−103.
(12) Liu, J. H.; An, J. W.; Ma, Y. X.; Li, M. L.; Ma, R. B.; Yu, M.; Li, S. M. *Eur. Phys. J.−Appl. Phys.* **2012**, 57.
(13) Zhang, K.; Zhang, L. L.; Zhao, X. S.; Wu, J. S. *Chem. Mater.* **2010**, *22*, 1392−1401.
(14) Wang, H. L.; Hao, Q. L.; Yang, X. J.; Lu, L. D.; Wang, X. *ACS Appl. Mater. Interfaces* **2010**, *2*, 821−828.
(15) Yan, X.; Chen, J.; Yang, J.; Xue, Q.; Miele, P. *ACS Appl. Mater. Interfaces* **2010**, *2*, 2521−2529.
(16) Xu, J. J.; Wang, K.; Zu, S. Z.; Han, B. H.; Wei, Z. X. *ACS Nano* **2010**, *4*, 5019−5026.
(17) Wu, Q.; Xu, Y. X.; Yao, Z. Y.; Liu, A. R.; Shi, G. Q. *ACS Nano* **2010**, *4*, 1963−1970.
(18) Mao, L.; Zhang, K.; Chan, H. S. O.; Wu, J. S. *J. Mater. Chem.* **2012**, *22*, 80−85.
(19) Biswas, S.; Drzal, L. T. *Chem. Mater.* **2010**, *22*, 5667−5671.
(20) Kumar, N. A.; Choi, H. J.; Shin, Y. R.; Chang, D. W.; Dai, L.; Baek, J. B. *ACS Nano* **2012**, *6*, 1715−23.
(21) Otero, T. F.; Padilla, J. *J. Electroanal. Chem.* **2004**, *561*, 167−171.
(22) Tung, V. C.; Allen, M. J.; Yang, Y.; Kaner, R. B. *Nat. Nanotechnol.* **2009**, *4*, 25−29.
(23) Niyogi, S.; Bekyarova, E.; Itkis, M. E.; McWilliams, J. L.; Hamon, M. A.; Haddon, R. C. *J. Am. Chem. Soc.* **2006**, *128*, 7720−7721.
(24) Li, Z.; Chen, Y.; Du, Y.; Wang, X.; Yang, P.; Zheng, J. *Int. J. Hydrogen Energ* **2012**, *37*, 4880−4888.
(25) Villar-Rodil, S.; Paredes, J. I.; Martinez-Alonso, A.; Tascon, J. M. D. *Chem. Mater.* **2001**, *13*, 4297−4304.

(26) Yang, M.; Cao, K. Q.; Sui, L.; Qi, Y.; Zhu, J.; Waas, A.; Arruda, E. M.; Kieffer, J.; Thouless, M. D.; Kotov, N. A. *ACS Nano* **2011**, *5*, 6945−6954.
(27) Stejskal, J.; Sapurina, I.; Trchova, M.; Prokes, J. *Chem. Mater.* **2002**, *14*, 3602−3606.
(28) Baker, S. E.; Cai, W.; Lasseter, T. L.; Weidkamp, K. P.; Hamers, R. J. *Nano Lett.* **2002**, *2*, 1413−1417.
(29) Lomeda, J. R.; Doyle, C. D.; Kosynkin, D. V.; Hwang, W. F.; Tour, J. M. *J. Am. Chem. Soc.* **2008**, *130*, 16201−16206.
(30) Martsinovich, N.; Troisi, A. *Energy Environ. Sci.* **2011**, *4*, 4473−4495.